# Mechanistic Insight into 3-Deoxy-D-*manno*-octulosonate-8-phosphate Synthase and 3-Deoxy-D-*arabino*-heptulosonate-7-phosphate Synthase Utilizing Phosphorylated Monosaccharide Analogues†

David L. Howe,‡ Appavu K. Sundaram,‡ Jing Wu,‡ Domenico L. Gatti,§ and Ronald W. Woodard*,‡

*Department of Medicinal Chemistry, College of Pharmacy, University of Michigan, Ann Arbor, Michigan 48109-1065, and Department of Biochemistry and Molecular Biology, Wayne State University School of Medicine, Detroit, Michigan 48201*

*Received July 31, 2002; Revised Manuscript Received February 28, 2003*

ABSTRACT: *Escherichia coli* 3-deoxy-D-*manno*-octulosonate 8-phosphate (KDO8-P) synthase is able to utilize the five-carbon phosphorylated monosaccharide, 2-deoxyribose 5-phosphate (2dR5P), as an alternate substrate, but not D-ribose 5-phosphate (R5P) nor the four carbon analogue D-erythrose 4-phosphate (E4P). However, *E. coli* KDO8-P synthase in the presence of either R5P or E4P catalyzes the rapid consumption of approximately 1 mol of PEP per active site, after which consumption of PEP slows to a negligible but measurable rate. The mechanism of this abortive utilization of PEP was investigated using [2,3-$^{13}C_2$]-PEP and [3-F]-PEP, and the reaction products were determined by $^{13}C$, $^{31}P$, and $^{19}F$ NMR to be pyruvate, phosphate, and 2-phosphoglyceric acid (2-PGA). The formation of pyruvate and 2-PGA suggests that the reaction catalyzed by KDO8-P synthase may be initiated via a nucleophilic attack to PEP by a water molecule. In experiments in which the homologous enzyme, 3-deoxy-D-*arabino*-heptulosonate 7-phosphate (DAH7-P) synthase was incubated with D,L-glyceraldehyde 3-phosphate (G3P) and [2,3-$^{13}C_2$]-PEP, pyruvate and phosphate were the predominant species formed, suggesting that the reaction catalyzed by DAH7-P synthase starts with a nucleophilic attack by water onto PEP as observed in *E. coli* KDO8-P synthase.

The enzymes 3-deoxy-D-*manno*-octulosonate 8-phosphate (KDO8-P)[1] synthase and 3-deoxy-D-*arabino*-heptulosonate 7-phosphate (DAH7-P) synthase (phenylalanine-sensitive) catalyze the condensation of phosphoenolpyruvate (PEP) with D-arabinose 5-phosphate (A5P) and D-erythrose 4-phosphate (E4P), respectively (Scheme 1). In both enzymatic reactions, there appears to be a nucleophilic attack from the *si* face of $C_3^{PEP}$ onto the *re* face of the carbonyl of the respective phosphorylated monosaccharide (*1*−*3*). The generation of inorganic phosphate occurs by the cleavage of the C−O bond of the phosphate moiety of PEP (*4*, *5*).

In addition to catalyzing similar reactions, KDO8-P synthase and DAH7-P synthase have similar structural features and are now believed to have evolved from a common ancestor (*6*−*13*). However, while there are two distinct classes of KDO8-P synthases, one requiring a divalent metal and one not requiring a metal (*10*), all DAH7-P synthases studied to date require a divalent metal for catalysis. Examination of the crystal structures of the metallo-KDO8-P synthase from *Aquifex aeolicus* and of DAH7-P synthase from *Escherichia coli* reveals that in each enzyme the respective substrates bind similarly. For example, PEP binds at the bottom of the active site cavity in both enzymes (*9*, *14*). In the *A. aeolicus* KDO8-P synthase crystal structure, the phosphate moiety of the phosphorylated monosaccharide substrate is anchored near the surface of the enzyme with the carbonyl region projected into the active site in such a way that the *re* face of the carbonyl is facing the *si* face of $C_3^{PEP}$ (*9*). The published crystal structure of *E. coli* DAH7-P synthase does not have E4P bound in the active site. However, a sulfate ion was found bound near the surface of the enzyme at the same position as the phosphate moiety of the phosphorylated monosaccharide in KDO8-P synthase (*14*).

Despite extensive mechanistic and crystallographic studies (*2*, *3*, *5*−*9*, *11*−*22*), the molecular details of the first step in the condensation reaction catalyzed by either KDO8-P synthase or DAH7-P synthase remain unknown. On the basis of results from stereochemical studies and more recently crystallographic evidence, it has been proposed that the *A. aeolicus* (metallo) KDO8-P synthase and the DAH7-P synthase reactions are initiated by the nucleophilic attack of water onto the *si* face of $C_2^{PEP}$ (*8*, *9*, *12*, *23*) (Figure 1, path a). Asojo et al. have proposed that the *E. coli* (nonmetallo) KDO8-P synthase reaction is initiated by the formation of an oxocarbonium ion at $C_2^{PEP}$ (Figure 1, path b) (*13*). Regardless of which mechanism is operating, the carbon−carbon bond formation between the C3 of PEP and C1 of A5P must occur fast enought that rotation about the C2−C3 bond of PEP and the reaction would give rise to the same

† This investigation was supported by Public Health Service Grant GM 53069 (R.W.W.) and AI42868 (D.L.G.), awarded by the Department of Health and Human Services.

* To whom correspondence should be addressed.

‡ University of Michigan.

§ Wayne State University School of Medicine.

[1] Abbreviations: KDO8-P synthase, 3-deoxy-D-*manno*-octulosonate 8-phosphate synthase; DAH7-P synthase, 3-deoxy-D-*arabino*-heptulosonate 7-phosphate synthase; E4P, D-erythrose 4-phosphate; A5P, D-arabinose 5-phosphate; R5P, D-ribose 5-phosphate; 2dR5P, 2-deoxyribose 5-phosphate; PEP, phosphoenolpyruvate; 2-PGA, D-2-phosphoglyceric acid; G3P, D,L-glyceraldehyde-3-phosphate.

10.1021/bi026553z CCC: $25.00 
Published on Web 04/05/2003

Scheme 1: Overall Reactions for DAH7-P Synthase and KDO8-P Synthase

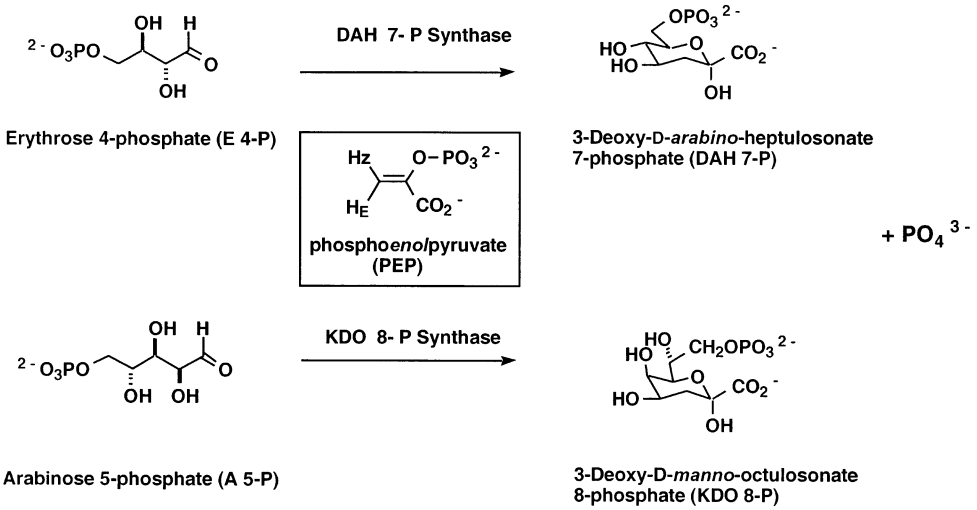


linear hemiketal bisphosphate intermediate (Figure 1). In the present study, the A5P substrate analogues, D-ribose 5-phosphate (R5P), 2-deoxyribose 5-phosphate (2dR5P), and E4P have been used to study the initial phase of the condensation reaction. New evidence supporting the view that a nucleophilic attack by water is indeed the first step in the *E. coli* KDO8-P synthase as well as in the *A. aeolicus* KDO8-P is presented.

Although E4P, 2dR5P, and R5P have been reported not to be alternate substrates for *E. coli* KDO8-P synthase (*24*), the crystal structures of the ternary complexes of *A. aeolicus* KDO8-P synthase with either PEP and E4P or PEP and R5P (*9*, *23*) suggest that both E4P and R5P might to able to bind in the active site of *E. coli* KDO8-P synthase, albeit in a noncatalytic mode. It should be noted from these reports that the crystal structure of *A. aeolicus* KDO8-P synthase alone contains two disordered loops that become ordered upon addition of both PEP and E4P or R5P. One can also envision with these saccharides that the *E. coli* KDO8-P synthase reaction would be initiated upon binding of both "substrates". After the ordering of the loops, the normal nucleophilic attack at $C_2^{PEP}$ would occur; however, the later stages of aldol condensation (namely, the attack of the $C_3^{PEP}$ onto C1 of the phosphorylated monosaccharide) would not proceed. The result would be a "trapped abortive-type intermediate" in the active site of *E. coli* KDO8-P synthase in which the first step(s) of the condensation reaction has occurred but not the later ones. Three different kinetic assays were utilized in this study to observe the events associated with each turnover (the conversion of PEP into KDO8-P and inorganic phosphate): (1) disappearance of the absorbance of PEP double bond (*25*), (2) formation of a 3-deoxymonosaccharide (*26*), and (3) release of inorganic phosphate (*27*, *28*). If R5P, 2dR5P, or E4P serves as an alternate substrate for KDO8-P synthase, then the rates determined with each of the three assays should be the same within experimental error. However, loss of PEP in the presence of any of these alternate saccharides without the concomitant formation of both the corresponding deoxymonosaccharide and inorganic phosphate would point to an alteration in one of the steps of catalysis. In addition, the data obtained from the studies with R5P (bearing the opposite stereochemistry of A5P at C2) and 2dR5P (totally lacking the C2 hydroxyl group of A5P) would provide insight into the role of the C2 hydroxyl group of the phosphorylated monosaccharide in the condensation reaction. The studies utilizing E4P would indicate the minimal length of the phosphorylated monosaccharide required for productive catalysis.

## MATERIALS AND METHODS

*Materials.* Phospho-*enol*-pyruvate mono(cyclohexylammonium) salt, A5P disodium salt, R5P disodium salt, E4P disodium salt, pyruvate sodium salt, D-2-phosphoglyceric acid (2-PGA) sodium salt, D,L-glyceraldehyde-3-phosphate (G3P), 2dR5P disodium salt, and L-lactate dehydrogenase (LDH) were obtained from Sigma Chemical Co. Puratronic $MnCl_2$ was purchased from Johnson Matthey. The sodium salt of [2,3-$^{13}C_2$]-pyruvate [99% $^{13}C$] was purchased from Cambridge Isotope Laboratories. The 1,3-bis[tris(hydroxymethyl)methyl amino]propane (BTP) and Tris base were obtained from Research Organics.

*Preparation and Purification of Recombinant E. coli KDO8-P Synthase.* KDO8-P synthase was prepared from *E. coli* BL21(DE3) cells harboring the pT7-7/*kds*A plasmid as previously described (*5*). Purified KDO8-P synthase was concentrated to approximately 35 mg/mL and stored at −80 °C.

*Preparation and Purification of Recombinant E. coli DAH7-P Synthase (Phenylalanine-Sensitive).* DAH7-P synthase was prepared from *E. coli* BL21(DE3) cells harboring the pT7-7/*aro*G plasmid as previously described (*20*). Purified DAH7-P synthase was concentrated to approximately 30 mg/mL and stored at −80 °C.

*Kinetic Methods. Monitoring the Disappearance of PEP's Double Bond.* The progress of the reaction was monitored using a continuous spectrophotometric assay to detect the loss of the double bond portion of the α,β-unsaturated carbonyl absorbance at $\lambda = 232$ nm ($\epsilon^{232} = 2840\ M^{-1}cm^{-1}$) at 37 °C (*16*). The final reaction mixture contained 100 mM Tris-acetate (pH 7.6), 150 μM PEP, and phosphorylated monosaccharide (values ranging from $0.1 \times K_m$ to $6 \times K_m$) in 1 mL total volume. The reaction was initiated upon addition of a 10 μL aliquot of KDO8-P synthase (1 μM final concentration). The reaction was mixed and monitored at 232 nm at 1 s intervals at 37 °C for a total of 2 min. The

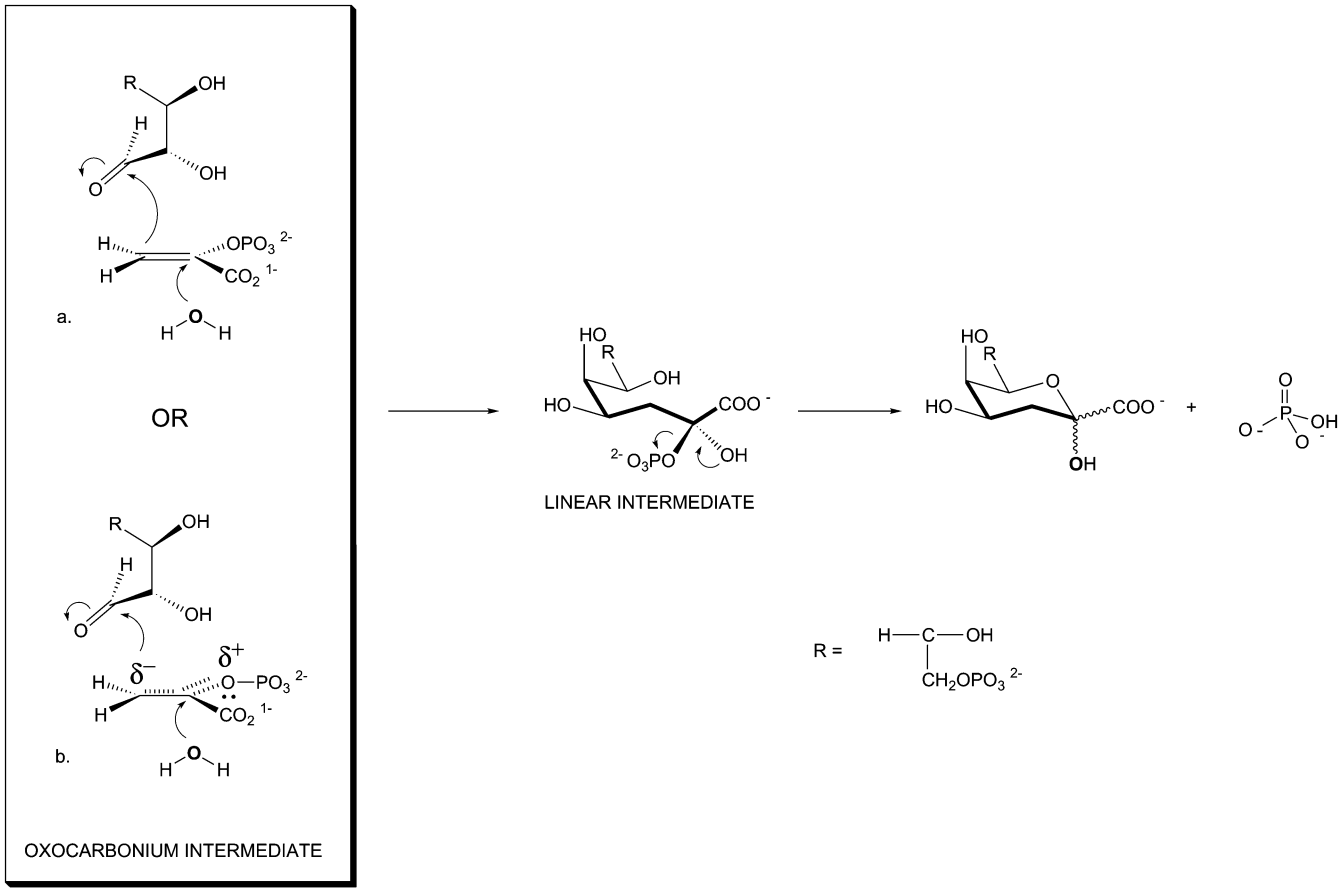


FIGURE 1: Proposed mechanisms for KDO8-P synthase (and DAH7-P synthase) proceeding through a linear hemiketal bisphosphate intermediate.

initial velocity was determined from a linear fit of the change in absorbance over 30 s of the reaction. $K_m$ and $V_{max}$ values for each phosphorylated monosaccharide were determined from a nonlinear regression fit of initial velocity as a function of phosphorylated monosaccharide concentration to the Michaelis−Menten equation using Kaleidagraph (version 3.08d).

*Determination of Release of Phosphate.* The extent of phosphate liberated from PEP during the course of reactions with phosphorylated monosaccharide was monitored utilizing a spectrophotometric assay based on a purine−nucleoside phosphorylase-coupled phosphate assay (*27*, *28*). In a total volume of 1 mL, the reaction mixture contained 100 mM Tris-acetate (pH 7.6), 150 $\mu$M PEP, 2 mM phosphorylated monosaccharide (R5P or E4P), 100 $\mu$M 7-methylinosine, 200 nM purine nucleoside phosphorylase (PNPase), and 1 $\mu$M KDO8-P synthase. The reaction mixture, minus KDO8-P synthase, was incubated at 37 °C for 3 min. The reaction was initiated by the addition of KDO8-P synthase and was monitored at 280 nm for 2 min at 1 s intervals. The conditions used for DAH7-P synthase assay have been previously described (*20*).

*Detection of the Formation of 3-Deoxymonosaccharides.* The amount of 3-deoxymonosaccharide product formed was determined using a modification of the Aminoff assay (*20*). The reaction mixture contained 100 mM Tris-acetate (pH 7.6), 3 mM PEP, 3 mM phosphorylated monosaccharide, and 1 $\mu$M KDO8-P synthase in a total volume of 50 $\mu$L. This reaction mixture was incubated at 37 °C for 10 min. The reaction was quenched by the addition of 50 $\mu$L of 10% trichloroacetic acid. The reaction mixture was subjected to the Aminoff assay, and the amount of 3-deoxymonosaccharide was determined [$\epsilon = 1.03 \times 10^5$ $M^{-1}cm^{-1}$ at 549 nm (*20*)]. The modified conditions used for DAH7-P synthase have been previously described (*20*).

*Large-Scale Enzymatic Synthesis of KDO8-P Analogues.* The procedures for the incubation of KDO8-P synthase (2 mg) with PEP and one of the phosphorylated monosaccharides as well as the purification of the products have been previously described (*20*).

*Enzymatic Synthesis of [2,3-$^{13}C_2$]-PEP.* The [2,3-$^{13}C_2$]-PEP was prepared using the enzyme pyruvate phosphate dikinase (a more than generous gift of Ms. Min Wei from the laboratory of Dr. Debra Dunaway-Mariano). The reaction mixture contained 50 mM $K_2HPO_4$, 50 mM ATP, 50 mM sodium [2,3-$^{13}C_2$]-pyruvate, 50 mM HEPES (potassium salt) (pH 7.0), 5 mM $MgCl_2$, 10 mM $NH_4Cl$, 20 units inorganic pyrophosphatase, and 25 units of pyruvate phosphate dikinase in a total volume of 4 mL. The reaction was incubated at room temperature (23 °C) for 2 days. An additional aliquot of inorganic pyrophosphatase (10 units) was added after the first day of incubation. The reaction products were separated from the enzymes using a Centriprep-20 ultrafiltration concentrator (Amicon). The filtrate was freeze-dried overnight and reconstituted into 4 mL of water. The [2,3-$^{13}C_2$]-PEP was purified by anion-exchange chromatography (AG-MP-1 column) using a linear gradient (0−0.5 M) of triethylamine bicarbonate buffer (pH 7.4). PEP-containing fractions were detected using a modification of the Malachite Green assay (*29*) where an 100 $\mu$L aliquot of the sample

was added to 900 $\mu$L of the malachite green−ammonium molybdate mixture and heated at 100 °C for 5 min. The sample was then cooled to room temperature. Fractions containing PEP remained a dark green after cooling to room temperature. The structure and isotopic content were confirmed using $^1$H NMR, $^{13}$C NMR, and $^{31}$P NMR spectroscopy. $^1$H NMR ($D_2O$, 500 MHz) $\delta$ 4.98 (d, 1H, $J$ = 5.4 Hz), 5.26 (d, 1H, $J$ = 1.8 Hz), 5.31 (d, 1H, $J$ = 5.3 Hz), 5.59 (d, 1H, $J$ = 1.9 Hz); $^{13}$C NMR ($D_2O$, 500 MHz) $\delta$ 104.17 (dd, $J$ = 81.3 Hz, $J$ = 3.8 Hz), 148.99 (m, $J$ = 81.3 Hz, $J$ = 8.0 Hz); $^{31}$P NMR (proton-decoupled, $D_2O$, 500 MHz) $\delta$ −3.04. The PEP-containing fractions were pooled, freeze-dried, and stored at −20 °C.

*NMR Studies of KDO8-P Synthase and DAH7-P Synthase (Phenylalanine-Sensitive). Procedure 1*. A reaction mixture containing 100 mM Tris-HCl (pH 7.4), 1 mM KDO8-P synthase, 1.5 mM [2,3-$^{13}C_2$]-PEP triethylamine salt, 1.0 mM phosphorylated monosaccharide (E4P or R5P), and $D_2O$ (10% v/v final concentration) in a total volume of 0.5 mL was incubated at 37 °C for 2 h. The progress of the reaction at 37 °C was monitored using $^{13}$C and $^{31}$P NMR (Bruker, Avance DRX 500 ($^1$H, 500.13235 MHz) with a 5 mm broad band probe. Phosphoric acid ($\delta$ = 0) was the external reference for $^{31}$P NMR spectra.

*Procedure 2*. A reaction mixture containing 100 mM Tris-acetate (pH 7.6), $D_2O$ (10% v/v), 0.032 mM KDO8-P synthase, 20 mM [2,3-$^{13}C_2$]-PEP triethylamine salt, and 60 mM E4P in a total volume of 0.5 mL was incubated at 37 °C for 2 h. Similarly, for studies with DAH7-P synthase, a reaction mixture containing 100 mM BTP-HCl (pH 6.8), $D_2O$ (10% v/v final concentration), 0.1 mM DAH7-P synthase, 20mM [2,3-$^{13}C_2$]-PEP, 60 mM G3P, and 1 mM $MnCl_2$ in a total volume of 0.5 mL was incubated at 37 °C for 2 h. The $^{13}$C and $^{31}$P NMR spectra were recorded for each reaction mixture (Bruker, Avance DRX 500 ($^1$H, 500.13235 MHz) with a 5 mm broad band probe.

*Enzymatic Detection of Pyruvate.* The presence of pyruvate in the enzyme reaction mixture was monitored using a coupled assay with L-lactate dehydrogenase (LDH) (*30*). The reaction mixture contained 100 mM Tris-HCl (pH 7.4), 150 $\mu$M PEP, 2 mM phosphorylated monosaccharide (R5P or E4P), 1 $\mu$M KDO8-P synthase, 100 $\mu$M NADH, and 18 U LDH in 1 mL total volume.

*Incubation of F-PEP and Phosphorylated Monosaccharide with KDO8-P Synthase.* A mixture of (*Z*)- and (*E*)-[3-F]-PEP (60:40) (*3*) was dissolved in 100 $\mu$L of 1 M Tris (pH 11) and 15 mg of phosphorylated monosaccharide (E4P or R5P) was added. The pH was adjusted to 7.4 using 1 M Tris and 50 $\mu$L of $D_2O$ was added to the solution. KDO8-P synthase (2 mg) was added and the volume was adjusted to 0.5 mL with water. The reaction mixtures were incubated at 37 °C, and the reaction progress was monitored by $^{19}$F NMR at various intervals for the first 24 h and every 24 h thereafter for 8 days. Trifluoroacetic acid ($\delta$ = 0) was the external reference for $^{19}$F NMR spectra.

*Inhibition of PEP Disappearance in the Presence of E4P or R5P*. KDO8-P synthase (180 nM) was incubated with various combinations of pyruvate, inorganic phosphate, 2-PGA, and either E4P or R5P. The combinations were as follows: E4P (1mM); E4P (1 mM) and pyruvate (1 mM); E4P (1 mM) and $P_i$ (1 mM); E4P (1 mM) and 2-PGA (1 mM); or E4P (1 mM), pyruvate (1 mM), and $P_i$ (1 mM). The incubation mixures contained 100 mM Tris-acetate (pH 7.6) in a total volume of 990 $\mu$L. Two sets of mixtures were prepared; one set was stored 23 °C and one set at 37 °C for 10 min. After 10 min, PEP (100 $\mu$M final concentration) was added to initiate the reaction. The disappearance of PEP was monitored as previously described. Each of the above experiments was repeated with R5P present instead of E4P.

*Protection Studies Against DEPC Inactivation of KDO8-P Synthase.* The ability of the phosphorylated monosaccharides and PEP to protect KDO8-P synthase (5 $\mu$M) against inactivation by diethylpyrocarbonate (DEPC) was evaluated. The phophorylated monosaccharide or PEP (100 $\mu$M final concentration) was incubated with KDO8-P synthase for 5 min at 23 °C prior to addition of 5 mM DEPC. After the addition of DEPC, aliquots (5 $\mu$L) were removed at various times, and the enzyme was assayed for residual activity using the thiobarbituric acid assay (*20*). Additionally, KDO8-P synthase (5 $\mu$M) was incubated with PEP (100 $\mu$M) and either R5P (100 $\mu$M) or E4P (100 $\mu$M) for 5 min at 23 °C before the addition of DEPC (5 mM). Aliquots (5 $\mu$L) were removed at various times and assayed for residual activity as described above.

*Computational Models.* All calculations were carried out using the program PC Spartan Pro (version 1.0.5, Deppmeier, B. J., Driessen, A. J., Hehre, W. J., Hehre, T., Klunzinger, P. E., Lou, L., and Yu, J. (2000) Wavefunction, Inc, Irvine, CA). The electron density, lowest unoccupied molecular orbitals (LUMO), and highest occupied molecular orbitals (HOMO) were calculated for PEP at the Hartree−Fock 6−31** level, and for (*Z*)- and (*E*)-[3-F]-PEP the semiempirical MNDO level was used. The geometry of the bound forms of PEP in the active site of *A. aeolicus* KDO8-P synthase (*9*) was used to determine the single-point energy for PEP and both (*Z*)- and (*E*)-[3-F]-PEP analogues. The hydrogen atoms at C-3 of PEP were added, and the resulting structure was minimized with all the atoms except the hydrogens held constant using PC Spartan Pro software. For the (*Z*)- and (*E*)-[3-F]-PEP compounds, the corresponding hydrogen atom was replaced by fluorine in silico. The resulting structure was again minimized, with all atoms except fluorine and hydrogen held constant. The electron density, lowest unoccupied molecular orbitals (LUMO), and highest occupied molecular orbitals (HOMO) were calculated for unbound PEP at the Hartree−Fock 6−31** level. The unbound PEP molecule was minimized using the PC Spartan Pro before calculations were performed.

## RESULTS

*Kinetics.* The substrate specificities of *E. coli* KDO8-P synthase with respect to the five carbon substrate analogues, R5P and 2dR5P, and the four carbon substrate analogue, E4P, were initially investigated by monitoring the disappearance of the absorbance due to the double bond of PEP (*16*). In the presence of 2dR5P, KDO8-P synthase appeared to catalyze the condensation reaction. The $K_m$ and $k_{cat}$ values for 2dR5P are given in Table 1.

On the basis of the observation of the rapid loss of absorbance at 232 nm over the initial 30 s of the reaction, KDO8-P synthase appeared to catalyze the condensation reaction between PEP and either R5P (Figure 2) or E4P (figure not shown). However, the disappearance PEP double

Table 1: Kinetic Parameters for KDO8-P Synthase Based on PEP Double-Bond Disappearance Assay[a]

| phosphorylated monosaccharide | $K_m$ ($\mu$M) | $k_{cat}$ ($s^{-1}$) |
|---|---|---|
| A5P[b] | $19 \pm 4$ | $6.8 \pm 0.5$ |
| E4P | $265 \pm 52$ | $0.28 \pm 0.02$ |
| R5P | $829 \pm 54$ | $(1.88 \pm 0.36) \times 10^{-2}$ |
| 2dR5P | $50 \pm 8$ | $0.12 \pm 0.05$ |
| arabinose | NS | NS |
| ribose | NS | NS |
| 2-deoxyribose | NS | NS |
| erythrose | NS | NS |

[a] The initial rates of PEP double bond loss were determined for *E. coli* KDO8-P synthase (1 $\mu$M) in the presence of PEP (150 $\mu$M) and various concentrations of the monosaccharides listed. The rates were modeled using the Michaelis−Menten equation. NS = not a substrate. [b] Previously determined using the PNPase assay (*20*).

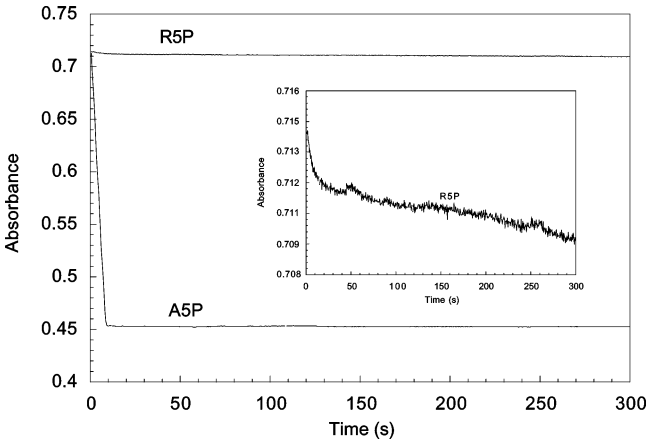


FIGURE 2: PEP double bond disappearance as a function of time. The rate of PEP double bond loss catalyzed by *E. coli* KDO8-P synthase (1 $\mu$M) in the presence of PEP (150 $\mu$M) and R5P (2 mM) or A5P (600 $\mu$M) in 100 mM Tris-acetate (pH 7.5) at a final volume of 1 mL as measured at $\lambda = 232$ nm. The inset shows an expansion of the plot for R5P.

bond over a period of 5 min appeared to be biphasic (the velocity of PEP disappearance for the rapid phase was 0.08 $\mu$M/s, while the slow phase was about 32 times slower at 0.0025 $\mu$M/s). As can be seen in the inset of Figure 2, there was a burst of PEP consumption that rapidly diminished after the consumption of approximately one-half to 1 equiv of PEP. Normal catalytic activity (turn over) was restored upon the addition of A5P to the reaction mixture after the initial burst of PEP loss was observed. The consumption of PEP (as monitored by the loss of absorbance at 232 nm) does not occur in the absence of R5P or E4P. The rate of loss of PEP double bond is dependent both on the amount of enzyme used and the concentration of R5P or E4P present. A plot of the rate of PEP double bond disappearance, during the first 30 s, as a function of R5P or E4P concentration was hyperbolic and could be modeled using the Michaelis−Menten equation although the values most likely contain the data from both reactions. The "apparent" $K_m$ and $k_{cat}$ values for R5P and E4P are given in Table 1.

On the basis of the observed disappearance of the PEP double bond, 2dR5P, R5P, and E4P all seem to behave as alternate substrates. However, when the formation and release of the reaction products was monitored utilizing the PNPase (phosphate release) and Aminoff assays (monosaccharide formation), only in the case of 2dR5P was there a clear

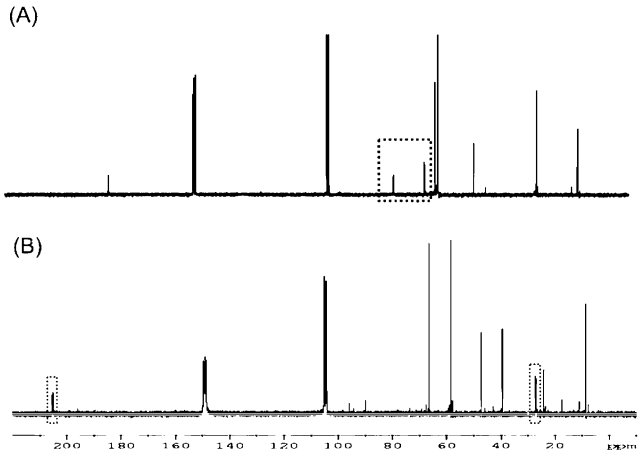


FIGURE 3: $^{13}C$ NMR spectra of KDO8-P synthase and DAH7-P synthase enzymatic reactions under saturating conditions. The reactions of KDO8-P synthase and DAH7-P synthases were monitored using $^{13}C$ NMR. (A) *E. coli* KDO8-P synthase with E4P and [2,3-$^{13}C_2$]-PEP present. A reaction mixture containing *E. coli* KDO8-P synthase (32 $\mu$M), E4P (60 mM), and [2,3-$^{13}C_2$]-PEP (20 mM) in 100 mM Tris-acetate (pH 7.6) at a total volume of 0.5 mL was incubated at 37 °C for 2 h. The reaction products were characterized using $^{13}C$ NMR. The absorbances due to 2-PGA formation are outlined. The peak at 26 ppm is due to the methyl group of the acetate portion of the Tris-acetate buffer. (B) *E. coli* DAH7-P synthase with G3P and [2,3-$^{13}C_2$]-PEP. A reaction mixture containing *E. coli* DAH7-P synthase (32 $\mu$M), G3P (60 mM), [2,3-$^{13}C_2$]-PEP (20 mM), and $MnCl_2$ in 100 mM BTP-HCl (pH 6.8) at a total volume of 0.5 mL was incubated at 37 °C for 2 h. The reaction products were characterized using $^{13}C$ NMR. The absorbances due to pyruvate formation are outlined.

indication that a 3-deoxymonosaccharide and inorganic phosphate were generated and released from the active site. When either R5P or E4P was utilized as the monosaccharide, neither a 3-deoxymonosaccharide nor inorganic phosphate were detected (data not shown).

*Large Scale Enzymatic Synthesis of KDO8-P Analogues.* R5P, E4P, and 2dR5P were separately incubated with KDO8-P synthase in the presence of PEP for 2 h at 37 °C, and the reaction mixtures were purified using anion-exchange chromatography as described previously (*20*). The Aminoff assay was used initially to screen purified fractions for the formation of a 3-deoxymonosaccharide. For 2dR5P, Aminoff positive fractions were found to contain the corresponding 3-dideoxy-*gluco*(*manno*)-octulosonate 8-phosphate based on the $^1H$ NMR analysis (spectra not shown) (*20*). No Aminoff positive fractions were found when either R5P or E4P was incubated with PEP and KDO8-P synthase. In addition, all fractions were analyzed for the presence of phosphate species using the malachite green assay (*29*). The phosphate-containing fractions for each of the above mixtures were separately pooled and freeze-dried. $^1H$ NMR analysis of these fractions detected the presence of PEP and either R5P or E4P. Using [2,3-$^{13}C_2$]-PEP and KDO8-P synthase, these same reactions were repeated with E4P (Figure 3A) and R5P (not shown). The $^{13}C$ NMR analysis of the collected fractions for the E4P reaction revealed the presence of a new $^{13}C$-enriched fraction that eluted near PEP with chemical shift values of 75 and 65 ppm. The peaks at 185, 60, and 22 ppm are due to the buffer Tris-acetate.

*NMR Studies of KDO8-P Synthase with E4P and [2,3-$^{13}C_2$]-PEP.* The fate of [2,3-$^{13}C_2$]-PEP in the presence of E4P

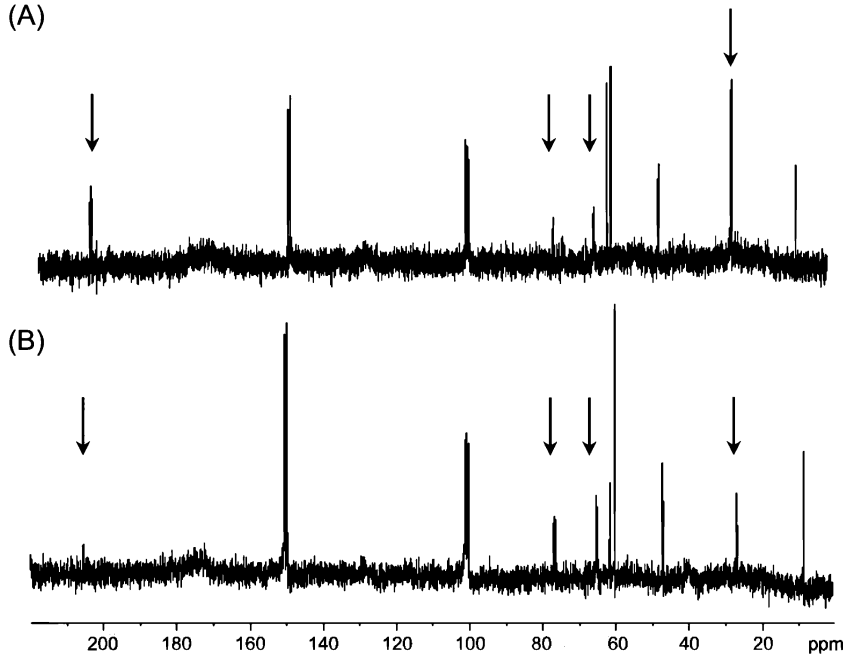


FIGURE 4: $^{13}C$ NMR spectra of *E. coli* KDO8-P synthase in the presence of [2,3-$^{13}C_2$]-PEP and either E4P or R5P under single-turnover conditions. (A) $^{13}C$ NMR spectra of *E. coli* KDO8-P synthase in the presence of 1.5 equiv of [2,3-$^{13}C_2$]-PEP and 1.0 equiv of E4P. The reaction mixture of *E. coli* KDO8-P synthase (1mM), [2,3-$^{13}C_2$]-PEP (1.5 mM), and E4P (1 mM) in 100 mM Tris-HCl (pH 7.6) at a total volume of 0.5 mL was incubated at 37 °C for 2 h. The reaction was monitored using $^{13}C$ NMR spectroscopy. (B) $^{13}C$ NMR spectra of *E. coli* KDO8-P synthase in the presence of 1.5 equiv of [2,3-$^{13}C_2$]-PEP and 1.0 equiv of R5P. The reaction mixture of *E. coli* KDO8-P synthase (1mM), [2,3-$^{13}C_2$]-PEP (1.5 mM), and R5P (1 mM) in 100 mM Tris-HCl (pH 7.6) at a total volume of 0.5 mL was incubated at 37 °C for 2 h. The reaction was monitored using $^{13}C$ NMR spectroscopy. Arrows denote resonances due to the formation of 2-PGA and pyruvate.

Table 2: $^{13}C$ NMR Data for KDO8-P Synthase with [2,3-$^{13}C_2$]-PEP and Either R5P or E4P Present under Single-Turnover Conditions

| compounds incubated with KDO8-P synthase | $\delta$ (ppm) | multiplicity of carbon |
|---|---|---|
| [2,3-$^{13}C_2$]-PEP | 150 | $-CH_2$ |
| | 105 | $-C$ |
| [2,3-$^{13}C_2$]-PEP + R5P | 27 | $-CH_3$ or $-CH$ |
| | 65 | $-CH_2$ |
| | 75 | $-CH$ or $-CH_3$ |
| | 208 | $-C$ |
| [2,3-$^{13}C_2$]-PEP + E4P | 27 | $-CH_3$ or $-CH$ |
| | 65 | $-CH_2$ |
| | 75 | $-CH$ or $-CH_3$ |
| | 208 | $-C$ |

[a] *E. coli* KDO8-P synthase (1 mM) was incubated with 1.5 equiv of [2,3-$^{13}C_2$]-PEP and 1 equiv of either E4P or R5P, as described under Materials and Methods. The multiplicity of carbon was assigned based on the corresponding DEPT-135 NMR spectra.

(stoichiometric quantities of enzyme−single turnover conditions) was monitored using $^{13}C$ NMR and $^{31}P$ NMR. Four additional $^{13}C$-resonances are present in the $^{13}C$ NMR spectrum (Figure 4A) and are given in Table 2. The multiplicities of these carbon atoms were further evaluated using a DEPT-135 pulse program (spectra not shown) and are summarized in Table 2. The $^{13}C$ NMR and DEPT-135 spectra are consistent, with pyruvate ($\delta = 27$ and 208 ppm) and 2-PGA ($\delta = 65$ and 75 ppm) formation occurring. The assignments of the resonances were confirmed using an external standard of either 10 mM [2,3-$^{13}C_2$]-pyruvate or 10 mM 2-PGA dissolved in reaction buffer. Inclusion of KF (10 mM), a known inhibitor of enolase activity, in the enzyme reaction mixture resulted in no observable change in the $^{13}C$ NMR spectra as compared to the reaction without KF present.

After the addition of E4P, there are four phosphate signals present in the $^{31}P$ NMR spectra (Figure 5A). Two of the phosphate resonances corresponded to the starting materials (PEP and E4P), while the two new phosphate resonances corresponded to 2-PGA and inorganic phosphate. The assignments of inorganic phosphate and 2-PGA were confirmed using an external standard of reaction buffer containing either 10 mM $KH_2PO_4$ or 10 mM 2-PGA.

*NMR Studies of KDO8-P Synthase with R5P and [2,3-$^{13}C_2$]-PEP.* The $^{13}C$ NMR spectra of KDO8-P synthase in the presence of R5P and [2,3-$^{13}C_2$]-PEP (Figures 4B) indicated that pyruvate and 2-PGA formation occurred, as previously described for KDO8-P synthase in the presence of E4P and [2,3-$^{13}C_2$]-PEP. The $^{31}P$ NMR spectra (Figure 5B) indicate that 2-PGA and inorganic phosphate were formed, as was observed for KDO8-P synthase in the presence of E4P and [2,3-$^{13}C_2$]-PEP.

*Incubation of [3-F]-PEP and E4P with KDO8-P Synthase.* The reaction of a (60:40) mixture of (*Z*)- and (*E*)-[3-F]-PEP with E4P in the presence of KDO8-P synthase was monitored using $^{19}F$ NMR (Figure 6A). A new $^{19}F$-peak with a chemical shift (singlet at $\delta = -43.4$ ppm) upfield of the starting material ([3-F]-PEP) (doublets at $\delta = -65.3$ and $-76.8$) was observed. Addition of KF, as an internal standard, confirmed that the new fluorine resonance corresponds to $F^-$. The rate of formation of $F^-$, which occurs over a several day period, corresponds to the rate of disappearance of [3-F]-PEP (Figure 7A). The (*E*) isomer disappears faster than the (*Z*) isomer. Therefore, in the presence of E4P, KDO8-P synthase appears to display the same stereoselectivity for [3-F]-PEP, as previously reported for the reaction of [3-F]-PEP with A5P (*2*).

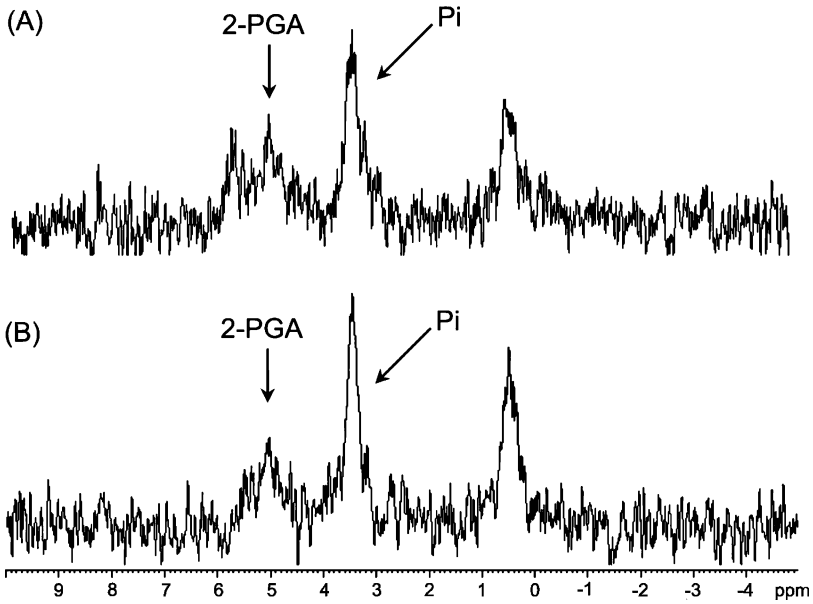


FIGURE 5: $^{31}$P NMR spectra of *E. coli* KDO8-P synthase in the presence of [2,3-$^{13}C_2$]-PEP and either E4P or R5P under single-turnover conditions. (A) $^{31}$P NMR spectra of *E. coli* KDO8-P synthase in the presence of 1.5 equiv of [2,3-$^{13}C_2$]-PEP and 1 equiv of E4P. The reaction mixture of *E. coli* KDO8-P synthase (1mM), [2,3-$^{13}C_2$]-PEP (1.5 mM), and E4P (1 mM) in 100 mM Tris-HCl (pH 7.6) at a total volume of 0.5 mL was incubated at 37 °C for 2 h. The reaction was monitored using $^{31}$P NMR spectroscopy. (B) $^{31}$P NMR spectra of *E. coli* KDO8-P synthase in the presence of 1.5 equiv of [2,3-$^{13}C_2$]-PEP and 1 equiv of R5P. The reaction mixture of *E. coli* KDO8-P synthase (1mM), [2,3-$^{13}C_2$]-PEP (1.5 mM), and R5P (1 mM) in 100 mM Tris-HCl (pH 7.6) at a total volume of 0.5 mL was incubated at 37 °C for 2 h. The reaction was monitored using $^{31}$P NMR spectroscopy.

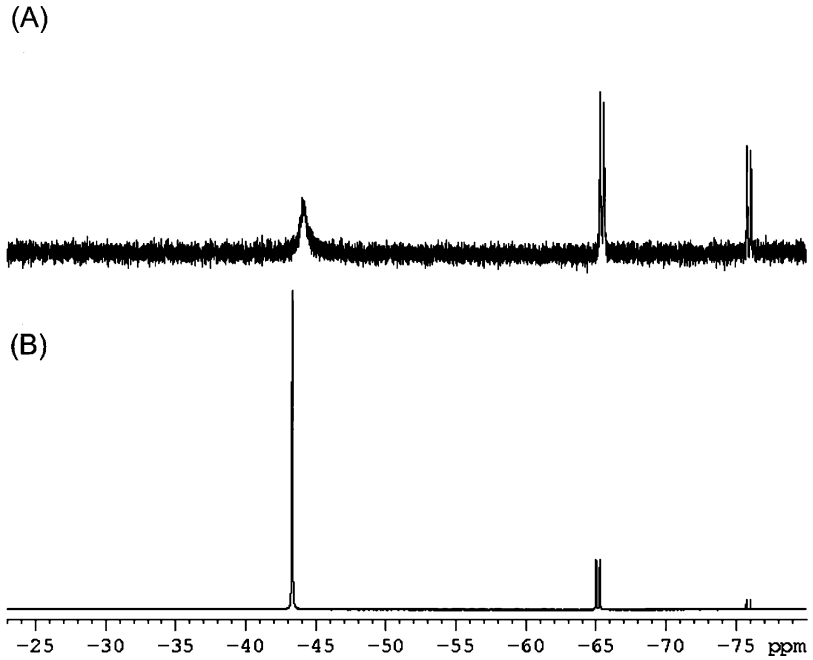


FIGURE 6: $^{19}$F NMR spectra of *E. coli* KDO8-P synthase in the presence [3-F]-PEP and either E4P or R5P under saturating conditions. (A) *E. coli* KDO8-P synthase with E4P and [3-F]-PEP present. A reaction mixture containing *E. coli* KDO8-P synthase (32 $\mu$M), E4P (60 mM), and a (60:40) mixture of (*Z*)- and (*E*)-[3-F]-PEP in 200 mM Tris (pH 7.4) at a total volume of 0.5 mL was incubated at 37 °C. The reaction was monitored using $^{19}$F NMR. (B) *E. coli* KDO8-P synthase with R5P and [3-F]-PEP present. A reaction mixture containing *E. coli* KDO8-P synthase (32 $\mu$M), R5P (60 mM), and a (60:40) mixture of (*Z*)- and (*E*)-[3-F]-PEP in 200 mM Tris (pH 7.4) at a total volume of 0.5 mL was incubated at 37 °C. The reaction was monitored using $^{19}$F NMR spectroscopy.

*Incubation of [3-F]-PEP and R5P with KDO8-P Synthase.* KDO8-P synthase was incubated with R5P and a 60:40 mixture of (*Z*)- and (*E*)-[3-F]-PEP. As was the case with E4P, $F^-$ was detected in the $^{19}$F NMR spectra (Figure 6B). The reaction occurred over several days (Figure 7B). As was previously described with E4P, KDO8-P synthase in the presence of R5P appeared to utilize the (*E*) isomer of [3-F]-PEP at a faster rate than the (*Z*) isomer (Figure 7B).

*NMR Studies of DAH7-P Synthase and D,L-glyceraldehyde-3-phosphate.* On the basis of the initial findings of the NMR investigation of KDO8-P synthase and E4P, the effect of G3P, a one-carbon shorter analogue of E4P, on the DAH7-P synthase reaction was investigated. DAH7-P synthase was incubated with G3P and [2,3-$^{13}C_2$]-PEP, and the progress of the reaction was monitored by $^{13}$C NMR. Under these conditions, DAH7-P synthase forms pyruvate but not 2-PGA

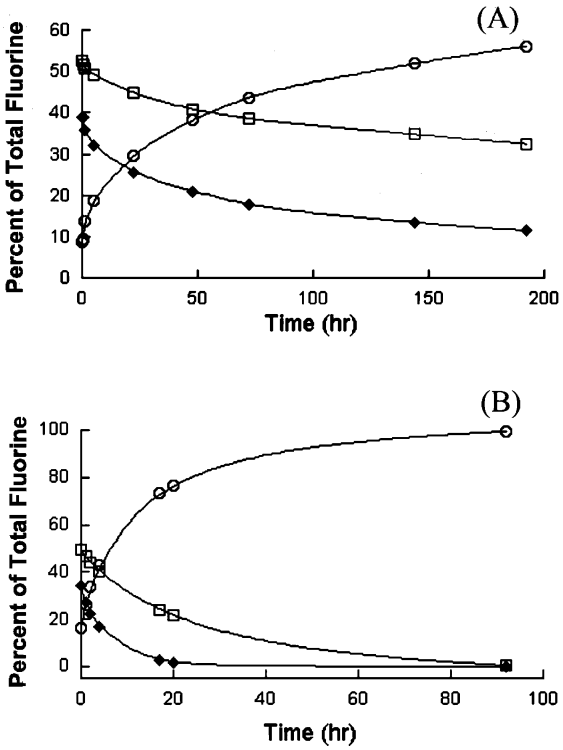


FIGURE 7: Rate of formation of $F^-$ by *E. coli* KDO8-P synthase in the presence of [3-F]-PEP and either E4P or R5P under saturating conditions. (A) *E. coli* KDO8-P synthase with E4P and [3-F]-PEP present. A reaction mixture containing *E. coli* KDO8-P synthase (32 $\mu$M), E4P (60 mM), and a (60:40) mixture of (*Z*)-[3-F]-PEP (□) and (*E*)-[3-F]-PEP (♦) in 200 mM Tris (pH 7.4) at a total volume of 0.5 mL was incubated at 37 °C. The reaction was monitored using $^{19}F$ NMR. (B) *E. coli* KDO8-P synthase with R5P and [3-F]-PEP present. A reaction mixture containing *E. coli* KDO8-P synthase (32 $\mu$M), R5P (60 mM), and a (60:40) mixture of (*Z*)-[3-F]-PEP (□) and (*E*)-[3-F]-PEP (♦) in 200 mM Tris (pH 7.4) at a total volume of 0.5 mL was incubated at 37 °C. The reaction was monitored using $^{19}F$ NMR spectroscopy. The corresponding absorbances for the product ($F^-$, $\delta = -43.4$ ppm) and the starting material ([3-F]-PEP $\delta = -65.3$ and $-76.8$ ppm) were integrated. The amount of $F^-$ formed is expressed as a percentage of the total area of $^{19}F$.

(Figure 3B). The remaining peaks in the spectra were present in the control spectra obtained in the absence of enzyme.

*Enzymatic Detection of Pyruvate with PEP and E4P or R5P.* The presence of "free" pyruvate in the enzymatic reaction mixtures was monitored with L-lactate dehydrogenase, which catalyzes the NADH-dependent reduction of pyruvate to lactate. No pyruvate formation could be detected when either E4P or R5P were incubated with PEP and KDO8-P synthase in the present of NADH and L-lactate dehydrogenase. Therefore, it appears that pyruvate is not released from the KDO8-P synthase complex, which is consistent with the finding that no inorganic phosphate was released from the same complex.

*Inhibition of PEP Disappearance in the Presence of E4P or R5P.* In the presence of E4P or R5P, the rapid disappearance of PEP appears to stop after one turnover. Preincubation of either phosphorylated monosaccharide and 2-PGA with KDO8-P synthase did not inhibit the initial burst of PEP consumption upon addition of PEP. Preincubation of either E4P or R5P with pyruvate again failed to inhibit the initial rate of double bond disappearance upon addition of PEP. The preincubation of inorganic phosphate and E4P or R5P, or pyruvate and inorganic phosphate with either E4P or R5P, failed to inhibit the initial burst observed upon the addition of PEP. The addition of 2-PGA, pyruvate, inorganic phosphate, and either E4P or R5P to the preincubation mixture did not inhibit the rapid turnover of PEP upon initiating the reaction with PEP. The initial turnover of PEP by KDO8-P synthase in the presence of either E4P or R5P could not be inhibited by preincubation of any of the proposed reaction products with KDO8-P synthase.

Table 3: Substrate Protection of KDO8-P Synthase against DEPC Inactivation[a]

| substrate added | fraction activity remaining |
|---|---|
| none | 0.07 |
| PEP | 0.68 |
| A5P | 0.37 |
| R5P | 0.15 |
| E4P | 0.40 |
| R5P + PEP | 0.85 |
| E4P + PEP | 0.87 |

[a] *E. coli* KDO8-P synthase (5 $\mu$M) was mixed with 100 $\mu$M of PEP, phosphorylated monosaccharide, or PEP and either R5P or E4P prior to the addition of 5 mM DEPC. After the addition of DEPC, aliquots (5 $\mu$L) were removed at various times and assayed for residual activity.

*Protection Against DEPC Inactivation of KDO8-P Synthase.* Preincubation of KDO8-P synthase with either PEP, E4P, A5P, or R5P alone offered protection against DEPC inactivation (Table 3). Protection from DEPC inactivation follows the trend PEP > E4P ≈ A5P > R5P. Preincubation of KDO8-P synthase with either PEP and E4P or PEP and R5P offered greater protection than the preincubation with PEP alone. The preincubation mixtures of PEP with E4P and PEP with R5P provided similar protection against DEPC inactivation (Table 3). The overall trend for the protection studies was PEP + E4P ≈ PEP + R5P > PEP > E4P ≈ A5P > R5P.

*Computational Studies.* The electron density, highest occupied molecular orbitals (HOMO), and lowest unoccupied molecular orbitals (LUMO) were calculated using the energy-minimized unbound conformation of PEP (Figures 8A and 8B), the enzyme-bound PEP conformations from the *A. aeolicus* KDO8-P synthase−PEP binary complex (Figure 8C,D), the *A. aeolicus* KDO8-P synthase−PEP−A5P ternary complex (Figure 9A,B), and the *A. aeolicus* KDO8-P synthase−PEP−E4P ternary complexes (Figure 9C,D) (*9*). The bending of PEP from planarity in the active site of the ternary complexes diminishes the positive charge found at $C_3^{PEP}$ and increases the positive charge on the *si* face of $C_2^{PEP}$ (Figures 8 and 9). Additionally, the electron density, HOMO, and LUMO calculations were conducted for (*Z*)- and (*E*)-[3-F]-PEP modeled into the active site of *A. aeolicus* KDO8-P synthase (not shown). The position of the fluorine does not dramatically alter the electronic environment of either $C_2$ or $C_3$ of [3-F]-PEP.

## DISCUSSION

The substrate specificity of *E. coli* KDO8-P synthase was investigated utilizing the phosphorylated monosaccharides, 2dR5P, R5P, and E4P. Crystallographic studies with the *A. aeolicus* metallo-KDO8-P synthase in complex with PEP and a phosphorylated monosaccharide have shown that E4P and

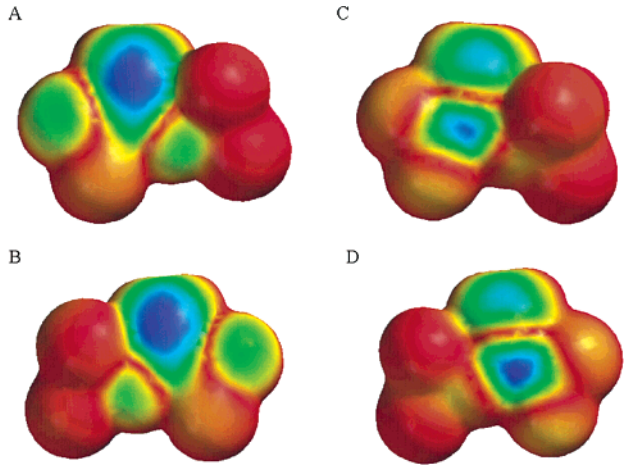


FIGURE 8: Calculated lowest unoccupied molecular orbitals (LUMO) projected on electron density maps of the (A) *re* face and (B) *si* face of energy-minimized PEP and (C) *re* face and (D) *si* face of PEP-bound to *A. aeolicus* KDO8-P synthase. LUMO were calculated using the Hartree−Fock 6−31** calculation model. Electron-rich areas are depicted in red, whereas electron deficient areas are represented in blue.

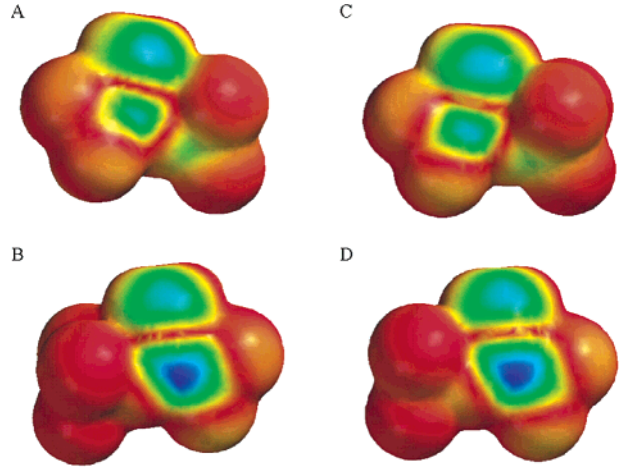


FIGURE 9: Calculated lowest unoccupied molecular orbitals (LUMO) projected on electron density maps of the (A) *re* face and (B) *si* face of PEP in the *A. aeolicus* KDO8-P synthase−PEP−A5P ternary complex and (C) *re*-face and (D) *si*-face of PEP in the *A. aeolicus* KDO8-P synthase−PEP−E4P ternary complex. LUMO were calculated using the Hartree−Fock 6−31** calculation model. Electron-rich areas are depicted in red, whereas electron deficient areas are represented in blue.

R5P bind in the active site in a way that is similar to A5P (*8*, *9*, *23*). The results of the DEPC protection experiment also verify that E4P and R5P bind into the active site of *E. coli* KDO8-P synthase in a manner similar to A5P. The incubation of *E. coli* KDO8-P synthase with E4P and PEP or R5P and PEP provided essentially the same protection against DEPC inactivation, which was greater than the protection provided by either E4P, R5P, or PEP alone (Table 3).

The A5P analogue, 2dR5P, but not R5P or E4P, was found to be an alternate substrate for KDO8-P synthase. However, in the presence of either E4P or R5P, KDO8-P synthase catalyzes the consumption of PEP in a biphasic manner without the formation of the respective phosphorylated monosaccharide products. There is an initial burst of PEP double bond loss that slows dramatically after a single turnover of KDO8-P synthase has occurred. The consumption of PEP appears to be catalyzed by KDO8-P synthase since E4P or R5P must be present for loss of PEP double bond to occur and the initial reaction rate is dependent on the concentration of KDO8-P synthase. Further examination of the fate of PEP under these conditions using $^{13}C$ NMR reveals that PEP is converted to pyruvate and 2-PGA by KDO8-P synthase in the presence of either E4P or R5P.

The formation of 2-PGA is particularly unexpected since a water attack at $C_3^{PEP}$ has never been postulated as part of the normal KDO8-P synthase reaction. The possibility of a contamination by the enzyme enolase, an enzyme that converts PEP to 2-PGA, can be ruled out because formation of 2-PGA by KDO8-P synthase is not inhibited by KF (a known inhibitor of enolase). Further, the conversion of PEP to 2-PGA by KDO8-P synthase only occurs in the presence of either E4P or R5P. The formation of 2-PGA was further investigated using [3-F]-PEP analogues. Stubbe and Kenyon previously conducted studies with enolase and [3-F]-PEP (*31*). Enolase utilizes [3-F]-PEP as an alternate substrate (*31*). They speculated that the 2-PGA fluoro analogue formed is unstable and decomposed into 3-oxo-2-phosphonoxypropionic acid and $F^-$ (*31*). We speculate that when KDO8-P synthase is incubated with [3-F]-PEP and either R5P or E4P that fluoro 2-PGA is formed as it was in the Stubbe and Kenyon enolase experiment. The appearance of $F^-$ in the $^{19}F$ NMR spectra of the above KDO8-P synthase reaction (Figure 6) provides additional evidence that KDO8-P synthase has a slow "enolase-like" activity. It should be noted that KDO8-P synthase catalyzes the condensation between [3-F]-PEP and A5P to give the corresponding 3F−KDO8-P analogues with the (*E*)-[3-F]-PEP reacting at a faster rate than (*Z*)-[3-F]-PEP (50% and 0.4% $V_{max}$, respectively) (*2*). The enolase activity of KDO8-P synthase in the presence of R5P or E4P shows the same trend with the (*E*) isomer consumed at a faster rate than the (*Z*) isomer of [3-F]-PEP (Figure 7). This would seem to further suggest that the enolase-like activity is due to [3F]PEP bound to the active site of KDO8-P synthase and not an enolase contaminant.

In the presence of either R5P or E4P, KDO8-P synthase catalyzes a nucleophilic attack of water at $C_2^{PEP}$ and an unusual attack by water at $C_3^{PEP}$ (Figure 10). The results of the $^{13}C$ NMR and $^{19}F$ NMR experiments indicate that 2-PGA formation occurs over many turnovers whereas pyruvate formation does not. The initial phase observed during the kinetic experiments, which appears to halt after approximately one turnover, can thus be assigned to pyruvate formation with the second "slower" phase being the formation of 2-PGA. The formation of 2-PGA was unexpected based on crystallographic studies with the KDO8-P synthase from the hyperthermophile *A. aeolicus* (*9*). A 2-PGA molecule was not observed in the crystal structures of *A. aeolicus* KDO8-P synthase in complex with PEP·E4P and PEP·R5P, which is what one would expect based on these results with the *E. coli* enzyme. However, a reexamination of the electron density of these *A. aeolicus* KDO8-P synthase complexes (Figure 11) reveals that 2-PGA formation may indeed have been observed. This reevaluation strengthens the case for the use of the *A. aeolicus* crystal structures as a tool for the understanding of the *E. coli* KDO8-P synthase catalytic mechanism.

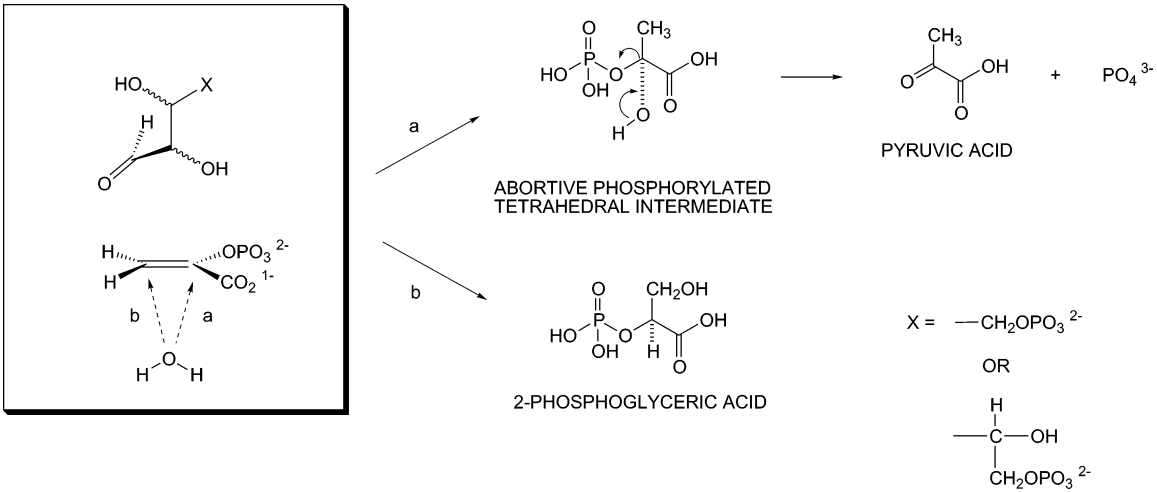


FIGURE 10: Proposed mechanisms for pyruvate and 2-PGA formation by *E. coli* KDO8-P synthase in the presence of PEP and either E4P or R5P.

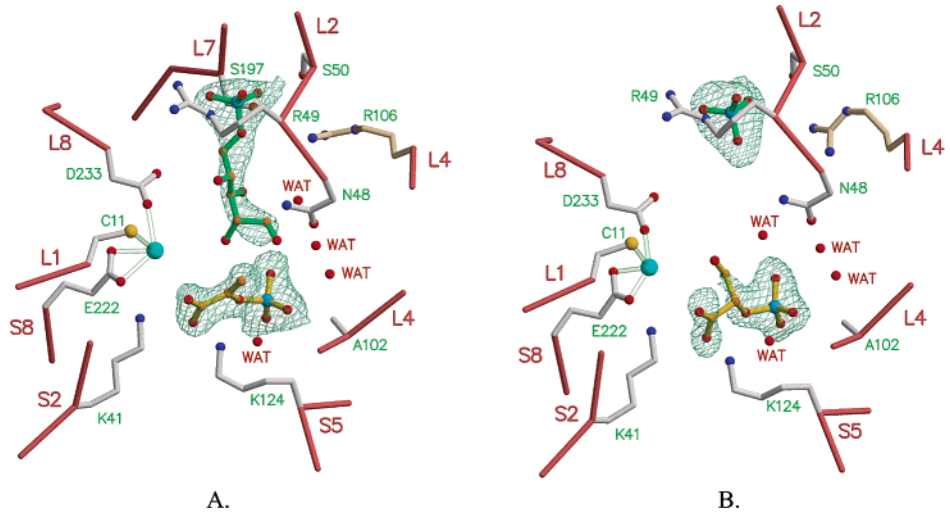


A. B.

FIGURE 11: *A. aeolicus* KDO8-P synthase active sites. In both panels the Cα trace and side chains of the enzyme are shown with salmon and white bonds, respectively. A single residue, Arg106, originating from a different monomer in the same asymmetric unit, is shown with kaki bonds. The coordination of the $Cd^{2+}$ ion is shown as transparent light green bonds. Nitrogen, blue; oxygen, red; carbon, orange; sulfur, yellow; phosphorus, pale blue; cadmium, cyan. (A) Active site in which both PEP and R5P bind. The electron density of PEP and R5P is shown contoured at 0.9 $\sigma$. (B) Active site in which R5P does not bind. A phosphate ion is bound at the position corresponding to the phosphate moiety of R5P in the other active site. The electron density of the other substrate is not well defined, and in this case it was interpreted as representing 2-PGA. Coordinates and electron density maps for this figure were derived from PDB entry 1JCY.

It is important to notice from the results of the kinetic studies, $^{19}F$ NMR, and large-scale enzymatic synthesis that while pyruvate production is completed after approximately a single turnover, 2-PGA formation continues during the course of the experiment. The conversion of PEP to 2-PGA is catalyzed by KDO8-P synthase and not contaminating enolase. Pyruvate and inorganic phosphate are not released from the active site, while 2-PGA is released into bulk solvent. When analyzed together, this information implies that there is cooperativity between the monomers in KDO8-P synthase. Indirect information on the type of conformational change/loop closure involved in this process can be gained from the crystal structures of *A. aeolicus* (metallo) KDO8-P synthase in complex with PEP-A5P, PEP·E4P, and PEP·R5P (*9*, *23*) (Figure 11). In these structures, each phosphorylated monosaccharide, E4P, A5P, or R5P, binds only in two active sites, whereas PEP binds in all four active sites. In the monomers with both the monosaccharide and PEP bound, the L7 loop (Figure 11) totally isolates the active site from solvent. In the other two monomers where only PEP is bound, the L7 loop is open, and the active site is in communication with the bulk solvent. Thus, the differences in pyruvate and 2-PGA formation rates may be explained based on the different conformations of the active sites in the two complexed states. Binding of R5P or E4P plus PEP to one face of the enzyme (two active sites) would trigger closing of the loop and the formation of pyruvate and inorganic phosphate, which are not released. This explanation is consistent with the failure to detect unbound inorganic phosphate and pyruvate using PNPase and LDH, respectively. Formation of 2-PGA would occur, instead, in the other two "semi-open" active sites containing only PEP (Figure 12). At these sites, bound PEP would eventually be hydrated to 2-PGA and released slowly until all the available substrate is utilized. This is exactly the situation observed in the [3-F]-PEP studies. Binding of A5P into the open active sites may trigger a conformational change in the enzyme, which opens the closed active sites containing pyruvate, inorganic phos-

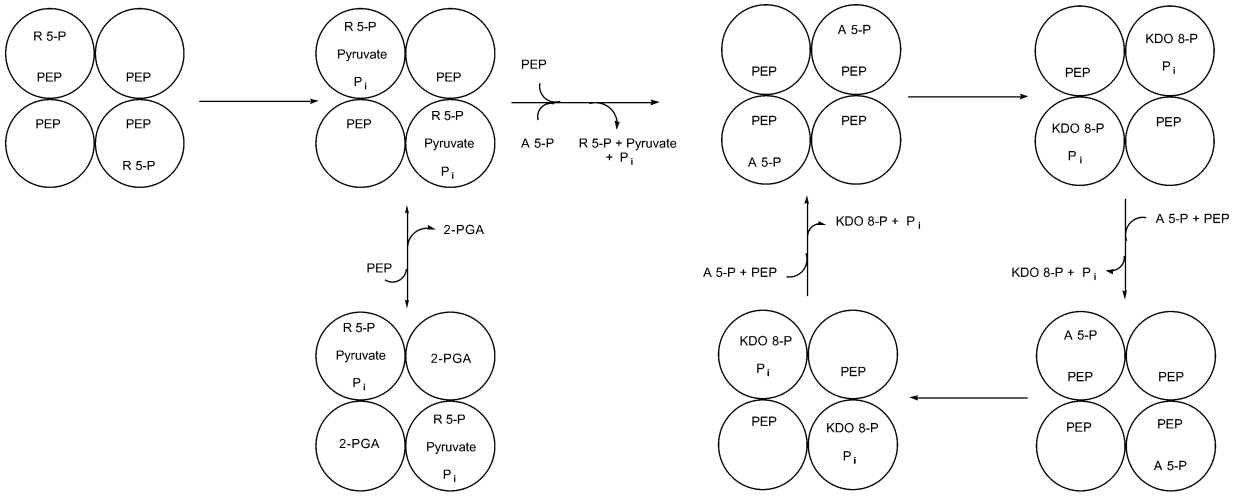


FIGURE 12: Schematic depicting (A) the abnormal (or abortive) reaction pathway in which PEP is bound to all four active sites of the tetrameric KDO8-P synthase and the phosphorylated monosaccharide is only bound in the two alternate active sites. In the two active sites with both "substrates" bound, very tightly bound pyruvate and phosphate are formed as determined by $^{13}C$- and $^{31}P$ NMR. The products are not released into bulk solvent. In the two sites with only PEP bound, KDO8-P synthase catalyzes an enolase-type reaction on the PEP. This is followed by the release of the 2-PGA from the active site. After the release of 2-PGA, another molecule of PEP binds into the same active site and is hydrolyzed to another molecule of 2-PGA. Panel B depicts the hypothesized normal pathway in which PEP binds to all four active sites. However, catalysis occurs only in alternate active sites in which A5P binds. The normal pathway maybe accessed from the abnormal or abortive pathway by the simple addition of A5P (see arrow between panels).

phate, and either R5P or E4P, allowing the release of the contents and restoration of normal KDO8-P synthase activity (Figure 12). Alternatively, formation of the proper condensation product may be the signal for the opening of the loops, and the abortive products may be incapable of eliciting the correct structural message that triggers loop opening.

The possible location of the water molecule attacking $C2^{PEP}$ with respect to the *re* or *si* face of this substrate was assessed by computational means. An analysis of the PDB coordinates for PEP in the *A. aeolicus* KDO8-P synthase ternary complexes indicates that a positive charge is located predominantly on the *si* face at $C_2^{PEP}$ (Figure 9). In both KDO8-P synthase·PEP·A5P and KDO8-P synthase·PEP·E4P ternary complexes, there is a water molecule on the *si* face of PEP in close proximity to $C_2^{PEP}$. However, in the KDO8-P synthase-PEP−R5P ternary complex this water molecule is not present. The kinetic data presented in this study are consistent with a direct role of this water in the condensation reaction. In fact, the rate of PEP double bond disappearance is 10-fold higher with E4P (the water is present) than with R5P (the water is absent).

The dihedral angle between the carboxylic acid and the double bond is increased upon the binding of A5P in the *A. aeolicus* KDO8-P synthase·PEP·A5P ternary complex (*9*). Density functional theory analysis (DFTA) indicate that increasing the dihedral angle between the carboxylate and $C_2^{PEP}$ increases the nucleophilicity of $C_3^{PEP}$ by increasing the HOMO density at $C_3^{PEP}$ (*32*). As predicted, the C-3 carbon appears to bend in the direction of the oxygen on the phosphate moiety of PEP upon the addition of A5P (*9*). This interaction may be the result of hydrogen bonding between the oxygen of the phosphate moiety and the (*Z*)-hydrogen at C-3 of PEP. The fluorine analogues of PEP, (*Z*)- and (*E*)-[3-F]-PEP, are utilized as alternate substrates in KDO8-P synthase (0.4% and 50% $V_{max}$ respectively) (*2*). The DFTA of the two fluorine PEP analogues suggests that the fluorine atom should not adversely affect the electronic environment of $C_2^{PEP}$ regardless of the stereochemistry of the PEP analogues. However, the (*Z*)-[3-F]-PEP would not be able to form a hydrogen bond with the oxygen of the phosphate moiety, whereas (*E*)-[3-F]-PEP is capable of forming a hydrogen bond. The ability to form this hydrogen bond may explain the preferential difference in activity between (*Z*)- and (*E*)-[3-F]-PEP.

KDO8-P synthase and DAH7-P synthase belong to the same protein family and are clearly the result of divergent evolution (*10*). Because of the similarities between these two enzymes, it seemed reasonable that a shorter E4P analogue, G3P, would produce, in DAH7-P, effects similar to those elicited by E4P in KDO8-P synthase. In fact, when DAH7-P synthase was incubated with G3P and PEP pyruvate was formed, clearly demonstrating that in DAH7-P synthase the initial step of the condensation reaction was also an attack by a nucleophilic water at $C_2^{PEP}$. Interestingly, 2-PGA was not formed when G3P and [2,3-$^{13}C_2$]-PEP were incubated with DAH7-P synthase. The most notable difference between these two enzymes was that DAH7-P synthase, but not *E. coli* KDO8-P synthase, required a divalent metal for activity. This observation suggests that the metal may play an important role in directing the attack of water exclusively onto $C_2^{PEP}$.

The results from this study and the *A. aeolicus* KDO8-P synthase X-ray crystallography studies (*9*, *23*) provide mechanistic details for KDO8-P synthase and DAH7-P synthase. The observed formation of pyruvate by KDO8-P synthase and DAH7-P synthase provides additional evidence supporting a nucleophilic attack by a water molecule onto $C_2^{PEP}$. This information does not distinguish between the

reaction being initiated through the transient formation of an oxocarbonium intermediate and the direct attack of water onto $C_2^{PEP}$. The formation of 2-PGA, while not on the normal reaction pathway, suggests that the reaction may, however, proceed through a direct attack by water and not through an oxocarbonium intermediate. The KDO8-P synthase "enolase" activity occurs only in the presence of PEP and either E4P or R5P not with PEP alone. On the basis of previous arguments, one face of the enzyme is locked in a conformation attempting to catalyze the normal reaction in the presence of PEP and either E4P or R5P, such that the loop overlooking the active site is closed and water begins the reaction by attacking the $C_2^{PEP}$. The other face contains only PEP and is awaiting the binding of the phosphorylated monosaccharide to continue the reaction cycle. The normal substrate, A5P, is able to restore normal catalytic activity suggesting that E4P and R5P may also be able to bind into the open face monomer-subunit containing PEP. The binding of E4P or R5P is not able to cause the necessary conformational changes for the correct nucleophilic attack by water onto PEP, but instead a nucleophilic attack by water at $C_3^{PEP}$ occurs. Clearly, additional mechanistic studies must be conducted to clearly elucidate the initial steps of the KDO8-P synthase and DAH7-P synthase reactions.

## REFERENCES


1. Dotson, G. D., Nanjappan, P., Reily, M. D., and Woodard, R. W. (1993) *Biochemistry 32*, 12392−7.
2. Kohen, A., Berkovich, R., Belakhov, V., and Baasov, T. (1993) *Bioorg. Med. Chem. Lett. 3*, 1577−82.
3. Sundaram, A. K., and Woodard, R. W. (2000) *J. Org. Chem. 65*, 5891−7.
4. Hedstrom, L., and Abeles, R. (1988) *Biochem. Biophys. Res. Commun. 157*, 816−20.
5. Dotson, G. D., Dua, R. K., Clemens, J. C., Wooten, E. W., and Woodard, R. W. (1995) *J. Biol. Chem. 270*, 13698−705.
6. Radaev, S., Dastidar, P., Patel, M., Woodard, R. W., and Gatti, D. L. (2000) *J. Biol. Chem. 275*, 9476−84.
7. Radaev, S., Dastidar, P., Patel, M., Woodard, R. W., and Gatti, D. L. (2000) *Acta Crystallogr. D56* (part 4), 516−9.
8. Duewel, H. S., and Woodard, R. W. (2000) *J. Biol. Chem. 275*, 22824−31.
9. Duewel, H. S., Radaev, S., Wang, J., Woodard, R. W., and Gatti, D. L. (2001) *J. Biol. Chem. 276*, 8393−402.
10. Birck, M. R., and Woodard, R. W. (2001) *J. Mol. Evol. 52*, 205−14.
11. Wagner, T., Shumilin, I. A., Bauerle, R., and Kretsinger, R. H. (2000) *J. Mol. Biol. 301*, 389−99.
12. Wagner, T., Kretsinger, R. H., Bauerle, R., and Tolbert, W. D. (2000) *J. Mol. Biol. 301*, 233−8.
13. Asojo, O., Friedman, J., Adir, N., Belakhov, V., Shoham, Y., and Baasov, T. (2001) *Biochemistry 40*, 6326−34.
14. Shumilin, I. A., Kretsinger, R. H., and Bauerle, R. H. (1999) *Structure 7*, 865−75.
15. Baasov, T., and Kohen, A. (1995) *J. Am. Chem. Soc. 117*, 6165−74.
16. Kohen, A., Jakob, A., and Baasov, T. (1992) *Eur. J. Biochem. 208*, 443−9.
17. Sheffer-Dee-Noor, S., Belakhov, V., and Baasov, T. (1993) *Bioorg. Med. Chem. Lett. 3*, 1583−8.
18. Sheflyan, G. Y., Duewel, H., and Woodard, R. W. (1999) *Biochemistry 38*, 14320−14329.
19. Howe, D. L., Duewel, H. S., and Woodard, R. W. (2000) *J. Biol. Chem. 275*, 40258−65.
20. Sheflyan, G. Y., Howe, D. L., Wilson, T. L., and Woodard, R. W. (1998) *J. Am. Chem. Soc. 120*, 11027−32.
21. Simpson, R. J., and Davidson, B. E. (1976) *Eur. J. Biochem. 70*, 501−7.
22. Liang, P. H., Lewis, J., Anderson, K. S., Kohen, A., D'Souza, F. W., Benenson, Y., and Baasov, T. (1998) *Biochemistry 37*, 16390−9.
23. Wang, J., Duewel, H. S., Woodard, R. W., and Gatti, D. L. (2001) *Biochemistry 40*, 15676−83.
24. Ray, P. H. (1980) *J. Bacteriol. 141*, 635−44.
25. Schoner, R., and Herrmann, K. M. (1976) *J. Biol. Chem. 251*, 5440−7.
26. Aminoff, D. (1961) *Biochem. J. 81*, 384−92.
27. Webb, M. R. (1992) *Proc. Natl. Acad. Sci. U.S.A. 89*, 4884−7.
28. Rieger, C. E., Lee, J., and Turnbull, J. L. (1997) *Anal. Biochem. 246*, 86−95.
29. Lanzetta, P., Alvarez, L. J., Reinach, P. S., and Candia, O. A. (1979) *Anal. Biochem. 100*, 95−7.
30. Schadewaldt, P., and Adelmeyer, F. (1996) *Anal. Biochem. 238*, 65−71.
31. Stubbe, J. A., and Kenyon, G. L. (1972) *Biochemistry 11*, 338−45.
32. Li, Y., and Evans, J. N. (1996) *Proc. Natl. Acad. Sci. U.S.A. 93*, 4612−6.


BI026553Z